MEASUREMENT OF DIELECTRIC PROPERTIES OF 3D PRINTED POLYMER-BASED MATERIALS FOR RF APPLICATIONS AT 500 MHz

P. Müller*, H. Hähnel
Institute of Applied Physics, Goethe University Frankfurt, Frankfurt am Main, Germany

Abstract

To include 3D printed polymer-based materials in accelerator parts, the relative permittivity and the dielectric loss tangent of these materials have to be well known. A quarter wave cavity was built to measure these properties at a resonance frequency of 500 MHz by inserting a cylinder of the material under test, resulting in a frequency and quality factor shift of the cavity. By fitting the measured data to detailed CST simulations, the values of the relative permittivity and the dielectric loss tangent can be obtained. These results provide the necessary material parameters for further investigations into their use in RF accelerator components such as power couplers.

INTRODUCTION

Metal 3D printing is already under investigation in linear accelerator components, enabling complex geometries that are almost impossible to manufacture conventionally [1–4]. In addition, consumer desktop 3D printers are widely used for fast prototyping, using polymer-based thermoplastic materials.The wide variety of polymer-based materials could also allow the use of these materials in linear accelerator components, such as RF power couplers, RF windows or in vacuum isolators. Therefore, it is important to estimate the dielectric properties of these materials, especially the relative permittivity ε_r and the dielectric loss tangent $\tan(\delta)$ are crucial parameters.For the common 3D printing materials such as PLA, PETG, and ABS, measurements of the relative permittivity were already performed at different frequencies [5–9]. Unfortunately, these materials have relatively low heat resistance compared to conventionally used materials such as ceramics (Al_2O_3) for this type of application, which motivates the investigation of advanced polymer-based materials.To estimate the values of the relative permittivity and the dielectric loss tangent a dedicated quarter-wave ($\lambda/4$) test cavity (see Fig. 1) was built from aluminum to achieve a high quality factor. The test cavity consists of three parts (inner conductor, tank, lid). A cylindrical test object made of the material under test induces a shift in frequency and quality factor of the test cavity. A comparison with detailed CST simulations yields the values of the relative permittivity ε_r and dielectric loss tangent $\tan(\delta)$ of the material under test.

SIMULATIONS

The dedicated quarter-wave test cavity in Fig. 1 was designed in CST Microwave Studio for a resonant frequency of 500 MHz. Due to tolerances in the manufacturing process, a corresponding simulation using the final dimensions was performed, yielding a resonance frequency of $f_0 = 499.627$ MHz and an unloaded quality factor of $Q_0 \approx 9746$.In CST, the contact resistance between the three parts was not taken into account, which is why the simulated quality factor is too optimistic. The real quality factor was measured and the CST simulation was adjusted to match this real quality factor of $Q_0 = 6127$. The measured resonance frequency $f_{0,\text{measured}} = 499.628$ MHz of the test cavity agrees with the simulated value within 1 kHz, indicating a good match between measurement and simulation.

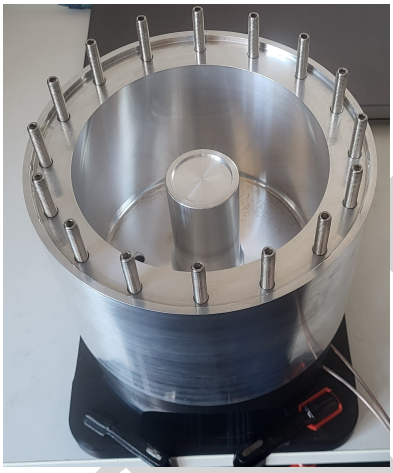

Figure 1: Final setup of the dedicated test cavity with removed top lid.

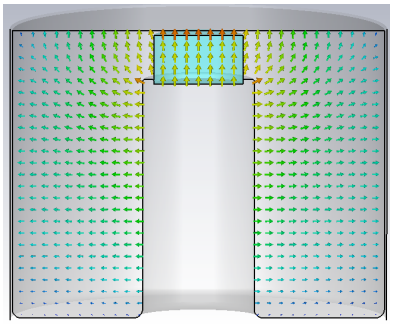

Figure 2: Cross-section of the CST model with a test object placed on the inner conductor. The arrows visualize the electric field inside the cavity.

Due to the quarter-wave ($\lambda/4$) structure of the test cavity, the electric field between the top of the inner conductor and the lid is approximately uniform; this region also exhibits the maximum field amplitude. A field disturbance caused by insertion of dielectric material in this region leads to a shift in resonance frequency and quality factor of the test cavity.A

* mueller@iap.uni-frankfurt.de

comparison of the simulated frequency and quality factor shift with the measured values yields the relative permittivity ε_r and the dielectric loss tangent $\tan(\delta)$. Therefore, a cylinder with a diameter of 40 mm and a height of 22 mm of the polymer-based material under test is placed on top of the inner conductor (see Fig. 2). In the simulation the relative permittivity of this cylinder is varied in the range of ε_r = 1.0 - 10.0, which was the expected range for common polymer-based filaments [5–8]. Figure 3 shows the result of this simulation, which allows to calculate the relative permittivity ϵ_r of the material under test, by measuring the frequency of the test cavity.

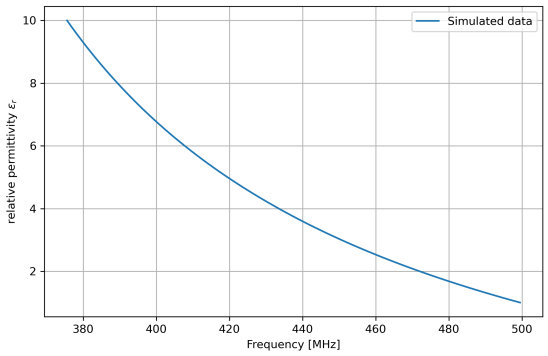

Figure 3: Simulated frequency of the test cavity in dependence of the relative permittivity ε_r of the test object.

To determine the dielectric loss tangent, the unloaded Q-value Q_0 is required, which can be calculated as [10]

$$Q_0 = \frac{2\pi f W}{P_C + \pi f \varepsilon_0 \varepsilon_r \int |\vec{E}|^2 dV \tan(\delta)}. \quad (1)$$

Here, W stands for the stored energy in the cavity and P_C for the surface (S) losses [10]:

$$P_C = \frac{1}{2}\sqrt{\frac{\pi \mu_0 \mu_r f}{\sigma}} \int |\vec{H_{tan}}|^2 dS. \quad (2)$$

The dielectric loss tangent $\tan(\delta)$ of the cylinder was varied in the CST simulation yielding a shift in quality factor of the cavity. With equation (1) the fit function for the dielectric loss tangent can be determined to

$$\tan(\delta) = \frac{\frac{a}{Q_0} - b}{c}. \quad (3)$$

Due to the relative permittivity dependency of the dielectric loss tangent in equation (1) the fit parameters have to be determined for each value of the relative permittivity.

EXPERIMENTAL SETUP

Test Cavity

The test cavity is made of aluminum to achieve a high quality factor. For repeatable measurements the inner conductor has a small ring to center the test cylinders. The final setup of the dedicated test cavity is shown in Fig. 1.

RF Coupling and Measurement

Coupling was achieved using small SMA sockets. Therefore, a thin copper wire is soldered to the inner conductor and through a hole in the SMA socket, also soldered to the outer conductor, forming a small coupling loop for inductive coupling. With small bends in the loop and rotation in the magnetic field, a weak coupling can be achieved, resulting in equality between the measured loaded and the unloaded Q-value ($Q_0 = Q_L$). An example of a coupling loop can be seen in Fig. 4.

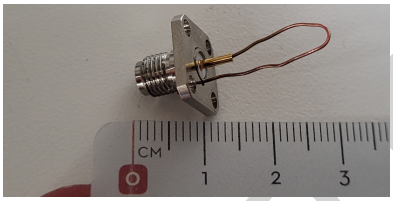

Figure 4: Example of a coupling loop connected to an SMA socket.

Test Objects

The different materials used in this study are polymer-based filaments which can be printed on modern desktop 3D printers. The printers used for this study were a BambuLab X1E and a H2C with maximum hotend temperatures of 320 °C and 350 °C respectively. Both printers have active chamber heaters up to 60 °C, which is also recommended for some of the materials. For commonly used standard materials in 3D-printing such as PLA, PETG, and ABS the default BambuLab printing profiles were used. For advanced materials such as PP, PA6-CF, and many others, the printing profiles of the manufacturer were used. If necessary, small adjustments were made to parameters such as printing temperature and printing speed. To ensure homogeneous parts with a good surface the BambuLab "Smooth PEI" plate was used on the X1E and the "Engineering" plate on the H2C. Figure 5 shows some of the 3D-printed test objects.

Figure 5: Some of the 3D-printed test objects which were used in the measurement.

MEASURED DATA

For the measurement itself a Rhode und Schwarz ZNB4 Network analyzer (NWA) was used. The measured resonance frequency and quality factor of the dedicated test cavity were averaged over ten measurements, which was set directly on the NWA. To improve the statistics, five test objects were measured for each data point and the results were

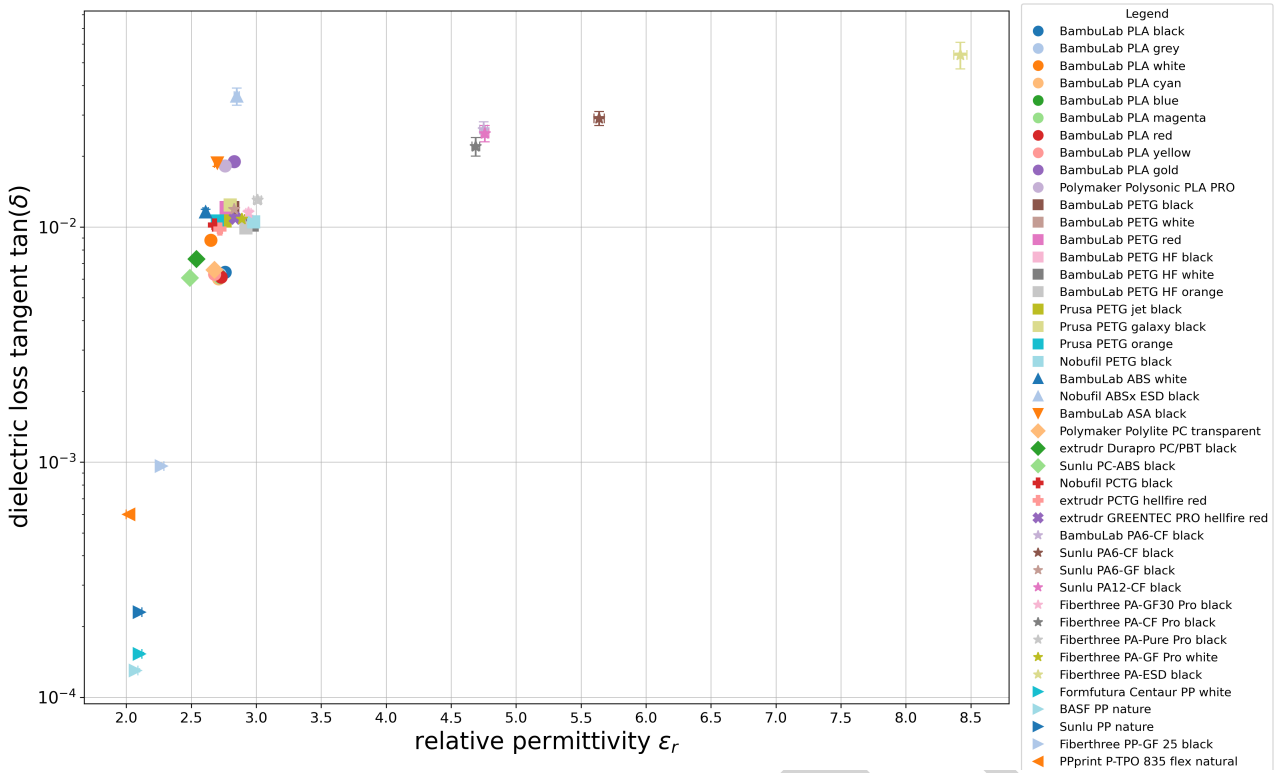

Figure 6: Measured relative permittivities ε_r and dielectric loss tangents $\tan(\delta)$ of the investigated polymer-based materials.

averaged. For the base materials, such as PLA, PETG, and ABS, only a single cylinder was used, due to their low heat resistance and the limited relevance of these materials for accelerator applications. The measured relative permittivities ε_r and the dielectric loss tangents $\tan(\delta)$ of a wide range of 3D printable polymer-based materials are plotted in Fig. 6. The measured data show that most common materials, such as PLA, PETG, and ABS have relative permittivities ε_r in the range of 2.5 - 3.0. However, the different PA types exhibit comparatively high relative permittivities, while their dielectric loss tangents are in the same order of magnitude as those of PLA, PETG, and ABS ($\tan(\delta) \sim 10^{-3}$ - 10^{-2}), which is comparatively high for applications in RF-accelerators. Interestingly, PP which has an ε_r of around 2.1, has a dielectric loss tangent $\tan(\delta)$ in the order of 10^{-4}, which is comparable or even lower than Al_2O_3 ($\tan(\delta) \sim 10^{-4}$) [11], which is a commonly used ceramics in RF power couplers. The main drawback of PP is its relatively low heat resistance, only allowing applications up to 41° [12], while Al_2O_3 can be used up to 1950° [11] in air.Within the measurements, different colors of PLA were used to investigate the influence of color on the relative permittivity and dielectric loss tangent. The results in Fig. 6 show, that the different colors slightly change the dielectric properties. The addition of carbon fibers (CF) or glass fibers (GF) alters the dielectric properties compared to the raw material.

CONCLUSION

The relative permittivity ε_r and dielectric loss tangent $\tan(\delta)$ of polymer-based materials used in desktop 3D printers were measured using a dedicated quarter-wave ($\lambda/4$) test cavity into which the material under test can be inserted. The presence of the sample results in frequency and quality factor shifts of this test cavity. A comparison of these shifts with detailed CST simulations yields the values of relative permittivity ε_r and dielectric loss tangent $\tan(\delta)$ of the tested materials. PP exhibited a comparatively low dielectric loss tangent ($\tan(\delta) \sim 10^{-4}$), but has low heat resistance, which restricts its use to low-power applications. The Fiberthree PP-GF 25 seems like a good candidate for further investigations. Due to the glass fiber reinforcement, the material exhibits significantly improved temperature resistance, allowing potential use in high-power applications.

ACKNOWLEDGMENTS

The authors would like to thank the companies Nobufil, Extrudr, Sunlu, Fiberthree, and PPprint for providing filaments used in this measurement.

REFERENCES

[1] H. Hähnel *et al.*, "Further high power tests of the additive manufacturing IH-type cavity", in *Proc. IPAC'25*, Taipei, Taiwan, Jun. 2025, pp. 1666–1669. doi:10.18429/JACoW-IPAC2025-WEAD3

[2] T. Romano *et al.*, "Metal additive manufacturing for particle accelerator applications", *Phys. Rev. Accel. Beams*, vol. 27, p. 054801, May 2024. doi:10.1103/PhysRevAccelBeams.27.054801

[3] T. Torims *et al.*, "Perspectives and recent achievements on additive manufacturing technologies for accelerators", in *Proc.*

IPAC'24, Nashville, TN, USA, May 2024, pp. 3890–3892. doi:10.18429/JACoW-IPAC2024-THPS62

[4] M. Mayerhofer *et al.*, "A 3D printed pure copper drift tube linac prototype", *Rev. Sci. Instrum.*, vol. 93, no. 2, p. 023304, 2022. doi:10.1063/5.0068494

[5] P. Parsons *et al.*, "Fabrication of low dielectric constant composite filaments for use in fused filament fabrication 3D printing", *Addit. Manuf.*, vol. 30, p. 100888, 2019. doi:10.1016/j.addma.2019.100888

[6] C. Dichtl *et al.*, "Dielectric properties of 3D printed polylactic acid", *Adv. Mater. Sci. Eng.*, vol. 2017, p. 6913835, 2017. doi:10.1155/2017/6913835

[7] D. Kalaš *et al.*, "FFF 3D printing in electronic applications: Dielectric and thermal properties of selected polymers", *Polymers*, vol. 13, no. 21, p. 3702, 2021. doi:10.3390/polym13213702

[8] N. Reyes *et al.*, "Complex dielectric permittivity of engineering and 3D-printing polymers at Q-band", *J. Infrared Millim. Terahertz Waves*, vol. 39, pp. 1140–1147, 2018. doi:10.1007/s10762-018-0528-9

[9] I. Kuzmanić *et al.*, "Influence of 3D printing properties on relative dielectric constant in PLA and ABS materials", *Prog. Addit. Manuf.*, vol. 8, pp. 703–710, 2023. doi:10.1007/s40964-023-00411-0

[10] Dassault Systèmes, "CST Studio Suite – User Manual", Version 2024, Darmstadt, Germany, 2024.

[11] Kyocera, "DEGUSSIT AL23 hf – Technical Data Sheet", Apr. 2023, accessed May 5, 2026.

[12] BASF, "Ultrafuse PP – Technical Data Sheet", Mar. 2020, accessed May 5, 2026.